Aerosol Monitoring by Satellite Horizon Scanning

C. R. GRAY,* H. L. MALCHOW,† D. C. MERRITT,† R. E. VAR†
Charles Stark Draper Laboratory, MIT, Cambridge, Mass.

A newly adapted horizon-scanning technique can simultaneously monitor the vertical distribution of aerosols, as well as ozone and neutral atmospheric density, in the stratosphere and mesosphere for both meteorological and ecological application in a global satellite-monitoring program. The horizon-inversion technique permits the conversion of scattered solar-radiation horizon (limb) profiles into the vertical distribution of aerosol extinction coefficients. Results are given based on real and simulated experimental data which indicate that the aerosol layers can be identified and that the potential exists for estimating the physical characteristics of aerosols within a layer.

Introduction

STRATOSPHERIC distributions of aerosols have been drawing increasing attention as a result of new knowledge concerning their role in the Earth's radiation balance. These particles are now known to cause temperature changes both in the stratosphere and at the Earth's surface. Of particular interest is the aerosol vertical distribution which is influenced both by man-made environmental pollutants and by natural phenomena.

This paper describes a mathematical technique of horizon-radiance inversion developed to recover the vertical distribution of aerosol extinction and, coincidentally, ozone and neutral atmospheric density in the stratosphere and mesosphere.[1] The technique provides for the inversion of horizon-intensity profiles obtained by scanning the Earth's sunlit horizon with a satellite-borne sensor. In this experimental configuration, a satellite-based sensor with a limited field of view mechanically scans the Earth's horizon (Fig. 1) in a multispectral mode, allowing the aerosols to be distinguished from other atmospheric constituents, such as the neutral atmosphere and ozone. The sensor output is inverted by applying a Kalman-Bucy recursive filter to the received signal, using a reference-intensity profile generated by a theoretical radiative-transfer simulation. When the scattering or absorption cross sections are well known (as in the case of ozone and the neutral atmosphere), the received multispectral signals are inverted to yield constituent-density information. When the cross sections are not well known, however—as in the case of aerosols—the extinction profile is obtained directly from the inversion. Further development of this horizon-inversion technique will permit determination of aerosol-scattering cross section and the associated size distribution in the stratosphere and mesosphere.

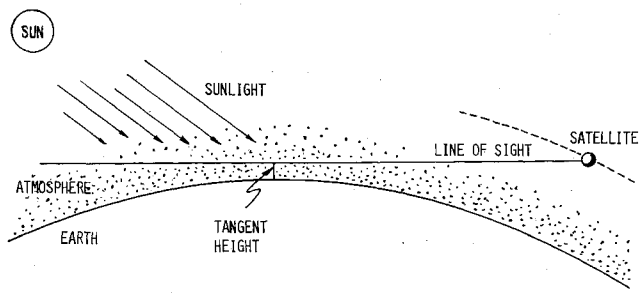

Fig. 1 Horizon-inversion geometry.

The horizon-inversion concept was chosen based on several considerations. Ground-based techniques are intrinsically insensitive to higher-altitude phenomena because of the overwhelming interference of the intervening atmosphere. The need arose, therefore, for satellite-borne remote sensors. The earliest ones, such as those carried by the Nimbus satellites, were downward-looking. However, since remote-sensing experiments have less spatial resolution along the line of sight than in the perpendicular direction, both ground-based vertical and satellite-based downward-looking experiments provide good horizontal resolution but relatively poor vertical resolution. This fact provided the impetus for the experimental configuration chosen here, in which the weakly-resolved direction is tangent to the Earth and the strongly-resolved direction (perpendicular to the line of sight) is along a local vertical. Thus, the horizon-inversion concept provides a highly accurate—and at the same time systematic—technique for global monitoring of the vertical distributions of various atmospheric constituents.

In this paper, the procedure for optimum wavelength selection is described, and convergence of the inversion model is discussed in relation to accuracies in the measurement model and the a priori knowledge of constituent densities. In addition, estimates of the inversion accuracy are given for the case of real experimental data, and also for simulated data generated by the radiative-transfer model.

Horizon-Inversion Technique

The following is a brief description of the horizon-inversion technique. Processed outputs from a multispectral photometer, which form a selected set of points along the horizon's tangent line of sight, are encoded and transmitted to the Earth. On the ground, a computer code compares the measured radiative intensity to a theoretical prediction; in proportion to the difference between measurement and prediction, the computer corrects previous estimates of the atmospheric-constituent densities, taking into account uncertainties in the a priori knowledge of the atmosphere and the various measurement noises. The procedure involves two primary mathematical structures—a radiative-transfer simulation for formulation of the theoretical prediction, and a recursive filter algorithm for treating the measurement noise and modeling errors. An abbreviated discussion of these two mathematical structures follows.

Radiative-Transfer Model

A variety of mathematical techniques has been applied to the calculation of theoretical horizon profiles, including layered iteration,[2] closed-form integration,[3] and Monte Carlo

Presented as AIAA paper 71-1111 at the Joint Conference on Sensing of Environmental Pollutants, Palo Alto, Calif., November 8–10, 1971; submitted November 30, 1971; revision received July 25, 1972.

Index category: Atmospheric, Space, and Oceanographic Sciences.

* Director, MIT Aeronomy Program, C.S. Draper Laboratory and Dept. of Meteorology.

† Staff engineer, MIT Aeronomy Program, C.S. Draper Laboratory.

simulation.[4] Some of these techniques have led to simulations involving the complex phenomenon of multiple scattering, while others have been limited to single-scattering approximation. For the actual application of the horizon-inversion technique,[1] a special computer code which uses weighted photon-path simulation is being developed; this code has demonstrated the potential of surpassing existing codes in accuracy and economy. However, to demonstrate the feasibility of the horizon-inversion technique, a less sophisticated transfer simulation can be employed, provided it maintains the general features of more comprehensive models and can be adjusted to match selected real data. A simulation that meets these requirements has been developed[5] and has been used to derive the results presented here.

The model used in the preliminary inversion analysis is a modified single-scattering solution to the equation of radiative transfer. Solar radiation scattered and absorbed along the receiver line of sight is integrated to obtain a single-scattered theoretical intensity. The single-scattered intensity is modified by albedo and multiple-scattering correction factors which are obtained by comparison with other, more accurate simulations. Values of the multiple-scattering factor depend upon sun angles, wavelength, and the tangent height for a particular measurement. The single-scattering model scales the directly scattered radiation according to the value of the aerosol or molecular angular scattering pattern which is taken as the leading element of the Mueller matrix.

The model gives the scalar intensity at the receiver as

$$I(m) = MS(m)[1 + A(m)]h(m) \tag{1}$$

where m = a given set of measurement parameters, i.e., wavelength, tangent height, solar zenith angle, etc., $MS(m)$ = a multiple-scattering correction factor, $1 + A(m)$ = an albedo correction factor with $A(m)$ equal to the fractional increase in the radiance caused by the surface albedo, and $h(m)$ = a single-scattering radiative-transfer equation integral. The integral $h(m)$ is defined as

$$h(m) = \int_{-\infty}^{L} J(\xi,m)e^{-\tau_s(\xi,m)}e^{-\tau(\xi;L,m)}d\xi \tag{2}$$

with τ_s = optical thickness of the curved atmosphere along the sun's ray path to the point ξ on the line of sight; τ = optical thickness along the line of sight from point ξ to the telescope; ξ = position along the telescope line of sight with zero taken at the tangent point; L = telescope position along the line of sight; and J = scattering source function.

The scattering source function is computed in the form

$$J(\xi,m) = F(m)\sum_i p_i(m)\sigma_{si}(m)\rho_i(\xi) \tag{3}$$

with F = solar irradiance, p_i = scattering phase function for the ith constituent, σ_{si} = scattering cross section for the ith constituent, and ρ_i = density of the ith constituent.

The calculation of radiance [Eq. (1)] is carried out by dividing the atmosphere into layers and expressing the integral [Eq. (2)] as sums over layered optical-depth increments. Partial derivatives of Eq. (1) with respect to constituent densities (which are used in the filter algorithm) are computed from the summation form of Eq. (1). A sample profile set generated by this model is displayed in Fig. 2.

The specific mathematical modeling of aerosols, which plays an important part in the inversion procedure, is defined in the following sentences. The data of Elterman[6] are used as the reference for the aerosol extinction at 5500 Å as a function of altitude up to 35 km. Above 35 km, the extinction is assumed to decrease exponentially with altitude at the same rate as neutral-density extinction. The basic curve of extinction at 5500 Å vs altitude is then scaled appropriately for wavelength and latitude. The wavelength dependence

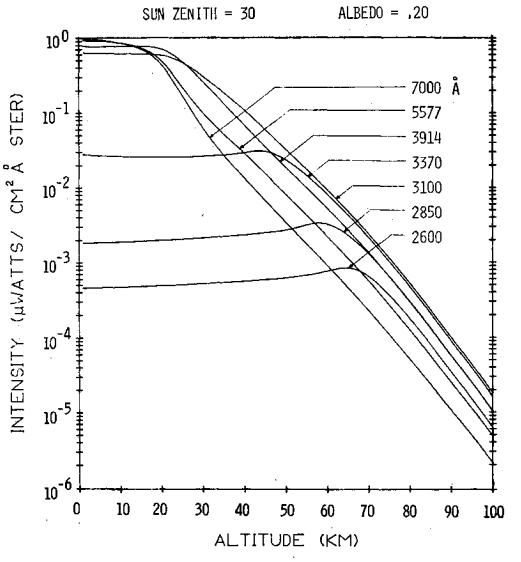

Fig. 2 Simulated horizon profile data.

is based upon an assumed particle size distribution. For this work, the power-law size distribution

$$n(r) = Ar^{-\alpha} \tag{4}$$

is used, where $n(r)$ is the number of particles at that radius, A is a total-density related constant, r is the particle radius, and α is the power-law parameter. Wavelength-correction factors for extinction have been determined for $\alpha = 3$ and $\alpha = 7$, with these two chosen as approximately the upper and lower limits of α values.

Recursive Filter

A modified extended Kalman-Bucy filter was used for the inversion process. This technique has a number of advantages: it can work easily with the complex solution to the equations of radiative transfer; it provides an optimal estimate of aerosol extinction and other constituent densities, considering both the measured data and initial statistics of the constituents; it provides a covariance matrix describing the second-order statistics of the optimal estimate.

In general, the extended Kalman-Bucy filter estimates the parameters or state (x) of a system, given measurements (y) of the system. The system in this application consists of the atmosphere and the measuring instrument. The modeled measurement equation for the system is

$$y(m) = I(x,m) + w \tag{5}$$

where $I(x,m)$ is a theoretically predicted value of the horizon radiance, m refers to the measurement-parameter wavelength and tangent height, and w is the instrument noise. The atmospheric state (x) is defined as a vector having as elements either the densities ρ or the extinction coefficients β of the atmosphere at a chosen set of altitudes z_i. Thus, for example, the state vector can be written as

$$\mathbf{x} = [\rho_N(z_1), \ldots \rho_N(z_n); \rho_O(z_1), \ldots \rho_O(z_n); \beta_A(z_1), \ldots \beta_A(z_n)] \tag{6}$$

The filter operates recursively by incorporating each new measurement of limb intensity at a particular tangent height and wavelength in an update of both the estimate of the state $\hat{\mathbf{x}}(m)$ and the covariance $P(m)$ associated with the estimate. The actual update is done in three steps: 1) Calculate the weighting factor or gain K of the filter

$$K(m+1) = P(m)B(m+1)^T[B(m+1)P(m)B(m+1) + R]^{-1} \tag{7}$$

where P,B, and R are defined below. 2) Incorporate the actual measurements y in an update of $\hat{\mathbf{x}}(m)$

$$\hat{\mathbf{x}}(m+1) = \hat{\mathbf{x}}(m) + K(m+1)[y - I(\hat{\mathbf{x}},m+1)] \quad (8)$$

3) Update the covariance matrix P to include the information gained from the measurement

$$P(m+1) = P(m) - K(m+1)B(m+1)P(m) \quad (9)$$

Equation (8) shows that the new optimal estimate $\hat{\mathbf{x}}(m+1)$ is equal to the old estimate $\hat{\mathbf{x}}(m)$ plus a weighting factor $K(m+1)$ times the difference between the predicted value of the measurement $I(\hat{\mathbf{x}},m+1)$ (based on the estimate of the state) and the actual value of the measurement y. The degree and distribution among the elements of x of the update depend upon three parameters. The first is the measurement-variance noise R. A noisy measurement will be lightly weighted. The second parameter is the covariance matrix P. Those elements of the state having small variances will be displaced proportionately less by the new measurement than elements which are poorly known. The third parameter is the measurement vector $B(m)$. This vector defines the contribution of each element of the state to the measurement. For example, constituents below the tangent height do not contribute significantly to the measured intensity, and thus the corresponding elements of $B(m)$ are nearly zero. $B(m)$ is defined as

$$B(m) = [\ldots,\partial y(m)/\partial x_i,\ldots] \quad (10)$$

The linear Kalman-Bucy filter assumes that B is independent of x_i for the scattered-light case; however, here $I(x,m)$ is nonlinear and it is necessary to work with the extended Kalman-Bucy filter. For the extended filter, the model measurement equation is expressed as

$$\Delta y(m) = B(x,m)\Delta x + w \quad (11)$$

where Δx is the difference between the state and a nominal estimate of the state. It can be seen from Eq. (11) that it is necessary to have an initial estimate of the state which is sufficiently close to the actual state at the time of the measurements to preserve the assumed conditions of linearity.

For most systems to which filters are applied, the state is a function of the measurement parameter—usually time, but in this case it is a function of a combination of wavelength and tangent height. Since $dx/dm = 0$ in this case, the filtering equations are somewhat simplified.

The filter requires an initial estimate of the statistics of the atmospheric state. Since little is known about the correlations between constituent densities, the covariance matrix is initially set with zero cross correlation. Variances are generally expressed as a constant fraction a of the densities; thus, initially

$$\mathrm{P_0} = \begin{bmatrix} \ddots & & 0 \\ & (ax_i)^2 & \\ 0 & & \ddots \end{bmatrix} \quad (12)$$

The filter described thus far assumes that the system behaves linearly about the initial estimate (i.e., the value of the measurement vector B is not functionally dependent on the estimate of the state), that the mathematical model of the system is exact, and that the measurements are made with an unbiased instrument. Few systems approximate these assumptions sufficiently well, however, and it is necessary to modify the filter program with techniques[7] which will ensure that the optimal estimate of the state will converge sufficiently close to the true state—even when these assumptions are not valid. The modifications depend in large part on the specific system, and can be determined only through extensive simulation. The techniques which were developed to improve the filter convergence for horizon inversion are described below.

The major obstacle to obtaining a convergent filter is the basic nonlinearity of the system. It was initially found in simulations that the filter could not converge if errors in any of the initial state element estimates exceeded 20%. This was an unacceptable constraint, since most aerosol densities may not be known to that degree of accuracy. The range of convergence of the filter was found, however, to be extendable to cases where initial state element estimates were in error by an order of magnitude or more through 1) damping the filter gain (at the cost of slower convergence) and 2) replacing the constituent densities with the log of the densities in the state vector. The latter technique improves the performance of the filter because it makes $B(m)$ more nearly independent of the state x.

The necessary modeling assumption of a layered atmosphere also interferes with the convergence of the filter. If the horizon-intensity data have a finer resolution than the vertical intervals assigned to the elements of the state, the filter will tend to "learn" one portion of the state too well, and will thus tend to overcompensate for the error in another portion of the state, causing the state to oscillate. This problem was handled by repeatedly sampling tangent-height data in altitude intervals compatible with those of the state, rather than handling each data point sequentially.

Various techniques have been applied to the treatment of biased measurements. These errors can be handled if the nature of the bias is known, for then it is possible to estimate the bias as an additional element of the state vector. The success of the technique depends primarily on the initial statistics ascribed to the densities and to the bias term. If the densities are reasonably well known, it is a simple matter to estimate the bias; and if the bias is well known, it is easy to estimate the densities. If both are poorly known, however, it is difficult to distinguish between an actual bias and a measurement bias. The filter does, however, provide an estimate of the bias and its uncertainty, which makes the confidence values for the final estimate of the densities realistic. The technique has been tested with reasonable success for the case of a bias error in tangent height.

Sensitivity

A central problem in horizon inversion is that of selecting wavelength channels which allow the probing of a particular atmospheric-constituent density over a selected altitude region. For example, one may be interested in the optimal channel for probing ozone in the 40–50 km region. A mathematical solution to this problem has been derived, and is labeled the "sensitivity" function. Values of the sensitivity function—or simply "sensitivity"—range from zero to unity, and larger sensitivities denote that fractional changes in constituent densities produce proportionally larger changes in the measured radiation signal. Since the information content for a particular constituent and altitude is reflected in a decrease in the variance asscociated with that element, it is natural to look at the covariance-update equation for the definition of sensitivity, namely

$$P(m+1) = P(m) - K(m+1)B(m+1)P(m) \quad (13)$$

The term of interest here is $K(m+1)B(m+1)P(m)$, which is the decrease in the covariance for a particular measurement condition. Normalizing by $P(m)$ yields a sensitivity matrix $K(m+1)B(m+1)$. Of particular interest in the sensitivity matrix are the diagonal elements which indicate the relative decrease in variance of the elements of the state vector for a given measurement. To isolate the effects of the measurement vector on the sensitivity, the instrument noise is assumed to be zero, and the covariance is assumed to maintain its initial value. With these assumptions, the sensitivity of the jth element of the state vector is defined as

$$s_j(m) = \left(\frac{\partial y(m)}{\partial x_j}\, x_j\right)^2 \Big/ \sum_i \left(\frac{\partial y(m)}{\partial x_i}\, x_i\right)^2 \quad (14)$$

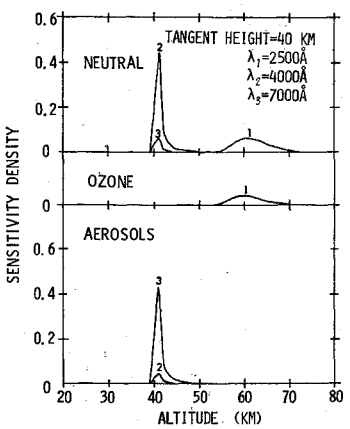

Fig. 3 Horizon-inversion sensitivity: 40-km line of-sight distribution.

For the purposes of the sensitivity analysis, the state vector is assumed to be defined at 1-km intervals. Figure 3 is an example of a plot of sensitivity vs altitude for neutral atmospheric density, ozone, and aerosols at a tangent height of 40 km and at wavelengths of 2500, 4000, and 7000 Å. These curves indicate that wavelengths around the ozone peak (2500 Å) do not penetrate below 50 km, whereas the longer wavelengths (4000 and 7000 Å) which are attenuated less by ozone have a peak sensitivity at the tangent height. This curve also indicates that 4000 Å is the optimal wavelength for determining neutral atmospheric density at 40 km, whereas 7000 Å is the optimal wavelength for aerosols.

Since the peak sensitivity usually occurs at the tangent height, it is convenient to analyze a complete limb scan by plotting peak sensitivity vs tangent height for the three constituents at various wavelengths. This is done in Fig. 4 for two values of the sun's zenith angle. The sun's azimuth angle is assumed to be zero (coplanar), and the zenith angle is defined relative to an Earth radius vector which is normal to the line of sight. A zenith angle of 90° means that the telescope is pointed directly at the sun.

In the sensitivity curves (Fig. 4), the relative constancy of the ozone sensitivity with zenith angle is the result of the fact that ozone is an absorber. The large variation in the aerosol and neutral atmospheric density sensitivities with zenith angle reflects, therefore, the relative changes in the scattering-phase functions for air and the aerosols assumed in the measurement model.

The peak in aerosol sensitivity around 20 km is related to the large concentration of aerosols between 35 and 20 km assumed in our atmospheric model. If ozone and aerosols had been neglected in the measurement model, the penetration altitudes for the neutral or Rayleigh constituents would continue to decrease with increasing wavelength, because of the λ^{-4} dependence of the Rayleigh-scattering cross section and the exponential distribution of neutral density. The presence of a strong ozone-absorption peak at 2550 Å, however, accounts for the general increase in penetration altitude as wavelength decreases below approximately 4000 Å or increases above 2000 Å toward the peak at 2550 Å.

Simulation Results

To adequately assess the performance of the horizon-inversion technique, a sequence of simulations was conducted. These simulations were performed to determine whether or not the inversion was performed adequately, since, in a simulation—unlike in the real experimental case—the actual value of the state is known beforehand. Therefore, if the actual value of the state falls within the rms limits about the final estimate of the state, the inversion has succeeded. Many simulations have been performed, and they indicate that bias errors, nonlinearities, and selected modeling errors can be adequately accommodated.

The results presented in Figs. 5 and 6 illustrate the capability of the inversion technique to determine anomalous aerosol layers under worst-case conditions of observability (i.e., when the sensitivities are low). In each of these figures, the aerosol extinction utilized in generating the simulated data is represented by the dotted line. The two solid lines represent the one-sigma values about the estimated extinction at each tangent altitude. These simulations were performed with a satellite altitude of 500 km, a ground albedo of 0.4, and instrument white noise with an rms value of 10^{-11} w/cm²-Å-sr, and wavelengths of 3000, 4000, 5000, 6000, and 7000 Å. Figure 5 is the result of a simulation with an anomalous $\alpha = 3$ aerosol layer placed at 20 km and a sun zenith angle of $-30°$ (corresponding to a scattering angle of 120°). Figure 6 is the result of a simulation with an anomalous $\alpha = 7$ aerosol

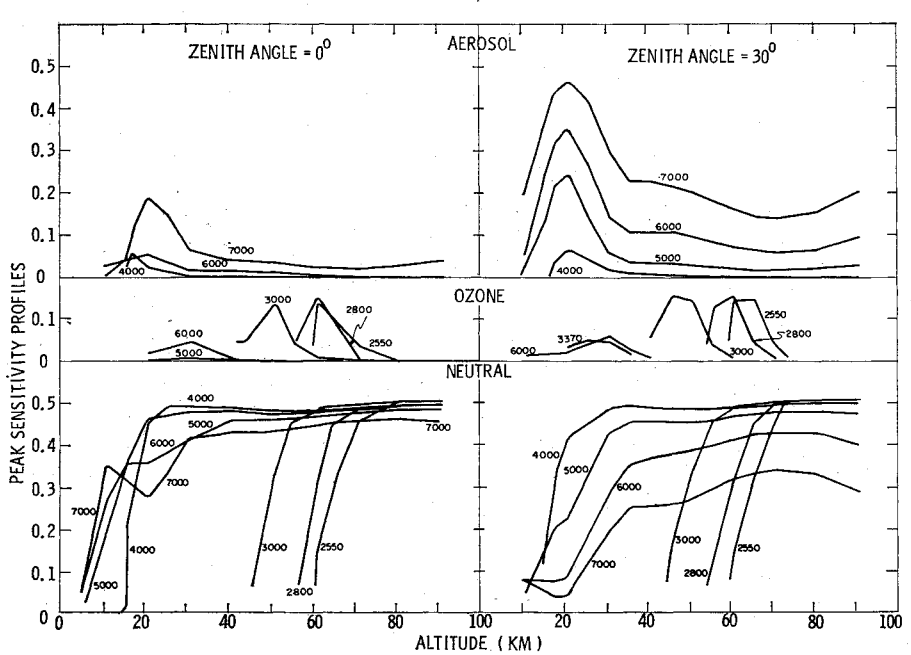

Fig. 4 Horizon-inversion peak sensitivity: zenith 0° and 30°.

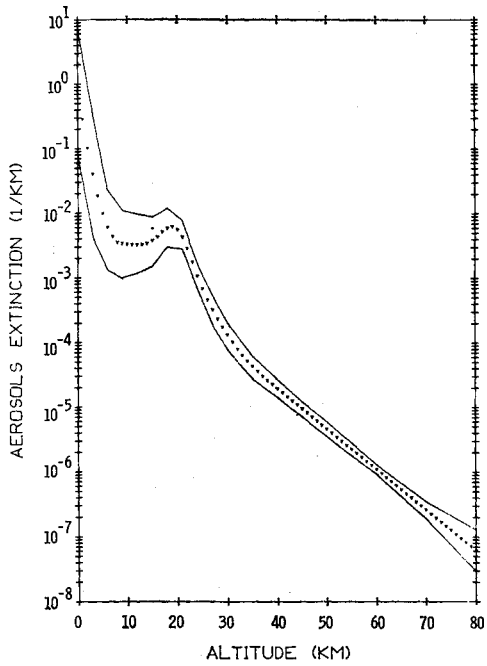

Fig. 5 Simulation results: inversion of 20 km, $\alpha = 3$ aerosol layer, zenith 30°.

layer placed at 50 km and a sun zenith angle of 60° (corresponding to a scattering angle of 30°).

The inversions shown in these simulation results were chosen because they represent two of the most difficult aerosol-inversion problems. In the first case (Fig. 5), the scattering phase function for the large size ($\alpha = 3$) aerosols has its smallest value for the scattering angle chosen (120°). In the second case (Fig. 6), it is difficult to differentiate between the Rayleigh scatterers and the small size ($\alpha = 7$) aerosol Mie-scatterers.

Since, in these figures, the actual value of the state indeed falls between the rms limits centered about the estimate of the state, it is clear that the inversion has succeeded extremely well under these adverse conditions. These results imply that a horizon-inversion experiment[1] will accurately determine the distribution of aerosols present in the stratosphere and mesosphere.

Since the aerosol size distribution causes changes in the wavelength dependence of the extinction, it is conceivable that this parameter, as well as all other wavelength-affecting aerosol parameters, can be determined by multispectral horizon scans simply by expanding the state vector to include these parameters. To estimate the expanded state, it is required only that there be as many measurements at each altitude as there are elements of the state at each altitude, and that the elements can be distinguished from each other by having different wavelength-dependent properties.

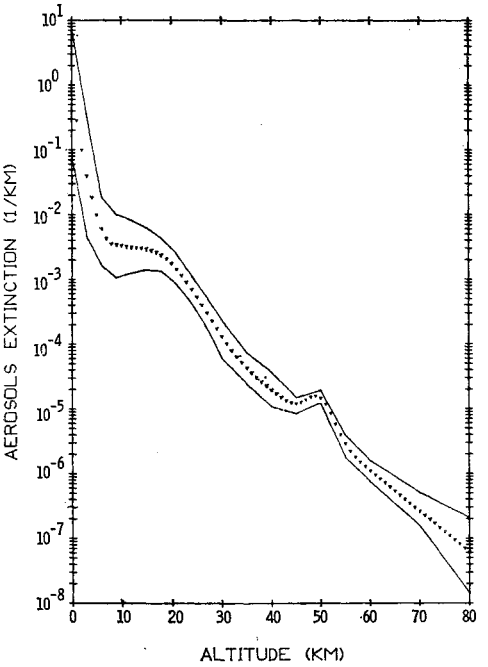

Fig. 6 Simulation results: inversion of 50 km, $\alpha = 7$ aerosol layer, zenith 60°.

Experimental Results

Application of the horizon-inversion formulations to the experimental horizon profiles for determination of the stratospheric and mesospheric distribution of aerosols has been most encouraging, considering the currently limited state of experimental horizon-profile data. The experimental data (Fig. 7) were obtained from a MIT experiment which defined the Earth's horizon for the purpose of extablishing Apollo navigation criteria.[8] A multispectral photometer mounted in the tail of the *X*-15-1 aircraft was flown on several occasions to heights of approximately 80 km, where a number of horizon scans were obtained. The scans at different wavelengths were performed sequentially as the *X*-15-1 ascended and descended in its ballistic trajectory, causing some loss of correlation between scans with regard to relative tangent-height positioning and cloud cover. The wavelengths were chosen at that time on the basis of navigation criteria, rather than inversion criteria; however, the sensitivity curves indicate that the selected wavelengths of 3500, 3800, 4200, 5800, and 7000 Å yield excellent information about neutral density and aerosols.

For inversions of these experimental results (Fig. 8), the inversion routine had a gain-damping of three, an instrument-noise level of 2.5×10^{-9} w/cm²-Å-sr, and a tangent-height increment spacing of 1 km. The data start at a tangent height of approximately 60 km and continue down to 15 km (below which level clouds significantly affect the signal). Confidence in the accuracy of these final results can be acquired by comparing the inversion estimate of neutral density with a reference value of neutral density, which is a good base line, since neutral density is reasonably well known. The mean neutral density at all altitudes falls within the rms limits about the inversion estimate, indicating that the inversion estimates of neutral density and also, therefore, of the other constituents, are accurate to within their predicted rms limits. The rms limits are large, in this case, because

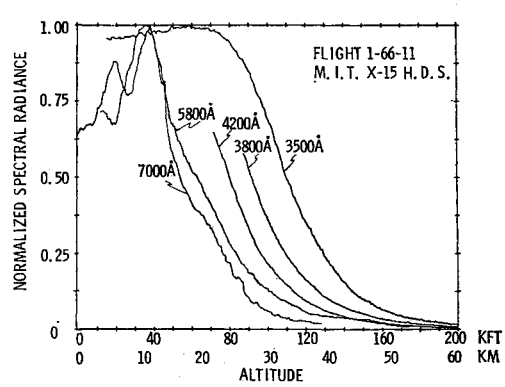

Fig. 7 *X*-15 normalized spectral radiance profiles: zenith 46°, scattering angle 106°.

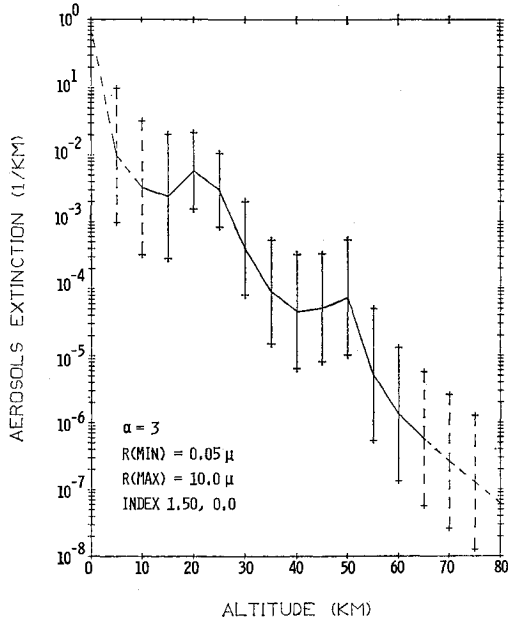

Fig. 8 Experimental results: inversion of *X*-15 data, aerosol extinction.

of the assumed large noise level and gain-damping factor, and because of the poor quality of these data and the modeling errors inherent in the single-scattering transfer model. The two aerosol layers at 25 km and 50 km are both real; although the rms values are large (0.5 in the log of estimation at 25 km and 0.8 in the log of estimation at 50 km), the estimated increases are even larger (0.7 in the log of estimation at 25 km and 1.2 in the log of estimation at 50 km). These two layers can both be seen in the raw data as increases in the *X*-15-1 horizon data at 5800 and 7000 Å. This 50-km layer is in general agreement with the layer recently measured[9] by a rocket-borne sensor at that altitude, and with the layer suggested by satellite measurements[10,11] of an anomalous increase in the backscattered ultraviolet intensity.

Conclusions

A satellite-borne, horizon-inversion experiment provides two significant advantages over other techniques for the monitoring of vertical distributions of aerosols in the upper atmosphere. First of all, the received signal is not encumbered by noise and attenuation produced by the lower atmosphere, and secondly, the altitude of an aerosol layer can be precisely located to within a fraction of a kilometer by means of highly accurate satellite ephemeris and attitude control.

Preliminary results show that aerosol layers can be identified with this procedure, and that the potential exists for estimating the physical characteristics of aerosols within a layer. The ultimate inversion accuracy obtainable from a limb-scan experiment lies somewhere between the results of the simulations and the uncertainties in the results of the *X*-15-1 data. In the final analysis, the accuracies in the radiative-transfer model, the predicted aerosol optical properties, and the radiance profile data will define the limitations on inversion accuracy. Although it is impossible to estimate final absolute accuracy, it seems reasonable to foresee that the use of a multiple-scattering model and simultaneous wavelength data will provide significant improvement over the inversion accuracies shown here for the *X*-15-1 data.

For meteorological purposes, these measurements are required to gain a better understanding of the energetics and dynamics of the upper atmosphere and its interaction with the lower atmosphere. For ecological purposes, these measurements would provide a capability for measuring the vertical distribution of stratospheric and mesospheric aerosols, thereby providing base-line environmental-pollution measurements globally for international consumption.

References

[1] Newell, R. E. and Gray, C. R., "Meteorological and Ecological Monitoring of the Stratosphere and Mesosphere," CR-2094, June 1971, NASA.

[2] Twomey, S., Jacobowitz, H., and Howell, H., "Matrix Methods for Multiple-Scattering Problems," *Journal of the Atmospheric Sciences*, Vol. 23, May 1966, p. 289.

[3] Chandrasekhar, S., *Radiative Transfer*, Dover, New York, 1960.

[4] Collins, D. and Wells, M., "Flash, A Monte Carlo Procedure for Use in Calculating Light Scattering in a Spherical Shell Atmosphere," AFCRL-70-0206, Jan. 1970, Air Force Cambridge Research Lab., Cambridge, Mass.

[5] Var, R. E., "A Hybrid Algorithm for Computing Scattered Sunlight Horizon Profiles," Internal Rept. AER 7-3, June 1971, Aeronomy Program, MIT, Cambridge, Mass.

[6] Elterman, L., "Vertical-Attenuation Model with Eight Surface Meteorological Ranges 2 to 13 Kilometers," AFCRL-70-0200, March 1970, Air Force Cambridge Research Lab., Cambridge, Mass.

[7] Jazwinski, A., *Stochastic Processes and Filtering Theory*, Academic Press, New York, 1970.

[8] Gray, C. R., "MIT/IL Horizon Definition Experiment Final Report," R-648, Oct. 1969, MIT Instrumentation Lab., Cambridge, Mass.

[9] Rossler, F., *Space Research VIII*, North-Holland, Amsterdam, Holland, 1968, p. 633.

[10] Elliott, D. D., "Effect of High Altitude (50 km) Aerosol Layer on Topside Ozone Sounding," *Space Research XI*, North-Holland, Amsterdam, Holland, 1971, pp. 857–861.

[11] Merritt, D. C., "The Application of a linear Recursive Filter to Nadir Ultraviolet Inversion," Internal Rept. AER 11-2, April 1971, Aeronomy Program, MIT, Cambridge, Mass.